Toluene removal from gas streams by an ionic liquid membrane: Experiment and modeling

Xueru Yan, Stéphane Anguille, Marc Bendahan, Philippe Moulin

Toluene removal from gas streams by an ionic liquid membrane: Experiment and modeling

Xueru Yan [a], Stéphane Anguille [b], Marc Bendahan [c], Philippe Moulin [a,*]

[a] Aix Marseille Univ., Centrale Marseille, CNRS, M2P2, Équipe Procédés Membranaires (EPM), Europôle de l'arbois, Bat. Laennec, Hall C, BP 80, 13545 Aix en Provence Cedex, France
[b] IUT Aix-Marseille, Dépt Chimie, 142 Traverse C. Susini, Marseille 13013, France
[c] Aix Marseille Univ., Université de Toulon, CNRS, IM2NP, AV. Escadrille Normandie Niémen, 13397 Marseille Cedex 20, France

ARTICLE INFO

Keywords:
Ionic liquid
Ceramic membrane
Toluene absorption
Operating conditions
Modelisation

ABSTRACT

Ionic liquids (ILs) are promising alternative solvents for traditional organic compounds using selective separation. However, some environmental risks of ILs, resulting in a limitation of their applications in industry. In this work, the stability of ILs into multi-channel tubular ceramic membranes (ILM) provides a promising way to realize the use of ILs with environmental damages reducing. This novel process has been investigated for toluene removal from a toluene/air gas mixture based on 1-butyl-3-imidazolium bis(trifluoromethylsulfonyl)amide ([Bmim][NTf_2]) as a liquid sorbent. In addition, the effects of operating conditions on toluene separation were studied and discussed by experiment and modeling. The absorption capacity of toluene by the ILM on proposed operating conditions was around 224.74 mg per gram of the ionic liquid. The support ceramic membrane can effectively prevent ILs leakage from causing secondary waste and ensure longtime operation. Regeneration of polluted ILM was available.

1. Introduction

Volatile organic compounds (VOCs), as a class of organic substances, are involved in several environmental pollutions and health damages. For example, the VOCs emission in the atmosphere causes environmental problems such as greenhouse effect, photochemical smog, and ozone depletion. For human health, VOCs are absorbed by the respiratory system, causing brain and liver damages [1–3]. It is necessary to reduce the emission of VOCs into the atmosphere. The current processes of VOCs abatement include destructive and recovery processes. Besides, recovery processes are more environmental-friendly. VOCs emissions control can be carried out in recovery processes such as adsorption on porous materials [4,5], membrane separation [6–8], condensation [9,10], and absorption by conventional solvents [11,12]. The selection of an efficient VOCs treatment process mainly depends on the concentration and flow rate of pollutants and the nature of compounds. Adsorption and absorption processes can treat much higher ranges of concentration and flow rate of pollutants than others [13]. Design and synthesis of porous materials for adsorption of VOCs such as metal organic frameworks [14–16], porous polymers [17–19], zeolites [20–22] and active carbon [23–26], has been extensively studied. However, this process may be limited when the gas flow with humidity. The presence of humidity has a noticeable impact on the adsorption of gases and volatiles [27–29]. Besides, because the moisture in the gas could block adsorption sites, it could be difficult to reuse the adsorbent [30]. The absorption process is the most simple and efficient for VOCs removal. In the absorption process, selecting an appropriate liquid absorbent is the key factor in achieving an effective and green separation process. Traditional organic solvents show the disadvantages of their not negligible volatility. A new solution, the addition of a nonaqueous solvent, has been found to enhance affinity for the solutes [30,31]. For example, silicone oils, solid polymers, and n-alkanes are widely used.

Recently, ionic liquids (ILs) have attracted wide attention as potential solvents to replace volatile organic solvents. The most important feature of ILs is the fact that they can dissolve both organic and inorganic compounds. Bedia et al. [30] confirmed that imidazolium-based ILs show better absorption capacities of toluene according to analyzing 272 types of ILs. As Table 1 shown, Rodriguez Castillo et al. [32] summarized the influence of the anion and cation structure of the IL on the toluene affinity. The type of anion, as a key factor, influences the solubility of ILs, and the length of the alkyl chain of the cation is also significant. Moreover, Gutel et al. [33] confirmed the interaction between toluene

* Corresponding author.
E-mail address: philippe.moulin@univ-amu.fr (P. Moulin).

Table 1
The influence of the anion nature and cation structure of the IL on the toluene affinity [32].

Parameter	Influence on the toluene affinity
Influence of the anion	$[NTf_2]$ > * $[PF_6]$ and [NfO]
Influence of the cation core	[Iq] with no ether function > [Morph] and [Triaz] > [im]
$-CH_3$ in the alkyl chain	+ with $[NTf_2]$ and imidazolium cation − with $[PF_6]$ and imidazolium cation
–CN in the alkyl chain	− with $[NTf_2]$ and imidazolium cation
Ether in the alkyl chain	ROC_2H_7 > $ROCH_3$ except with morpholinium cation

and the imidazolium-based IL, 1-butyl-3-imidazolium bis(trifluoromethylsulfonyl)amide ([Bmim][NTf_2]), from NMR and molecular simulations. Results showed that toluene is closer to the methyl group at the end of the butyl chain of [Bmim][NTf_2], resulting in relatively weak pi-interactions between aromatic substrates and the imidazolium ring of the IL. Moreover, the presence of H-bonding between the C_2-H and the anion in the [Bmim][NTf_2] generating a stronger association which results in toluene could not cleave the H-bond.

In this study, the imidazolium-based ionic liquid ([Bmim][NTf_2]) was used as the absorbent solution and combined with a tubular ceramic membrane for the absorption of VOCs from a gas stream. The porous ceramic membrane acts as a contacting device between the gas and liquid phase. The separation of the target gas (VOCs) relied on the solubility of the gas in the solvent (selected IL). Among VOCs, toluene is one of the most widely used gases in the industry [34,35]. Therefore, toluene, as a typical aromatic hydrocarbon, was captured as a model of VOCs.

2. Materials and methods

2.1. Vocs removal process

Toluene (100 ppm) – air mixture was purchased from Linde (Lyon, France). [Bmim][NTf_2] was purchased from Solvionic (Toulouse, France) without further purification. The ILM is a multi-channel ceramic membrane combing with ILs (Fig. 1). The support porous ceramic membrane was purchased from Alsys Society (Salidares, France). For this feasibility study commercial membrane was used. The influence of channel geometry on the ILM final separation performance is an interesting research topic but not develop in this paper as by Ghidossi et al. [36] for liquid filtration. The coating of the support membrane is a fluoropolymer that is conventionally used for the ends of the micro-ultra-nanofiltration membranes. A molecular weight cut off (MWCO) of 1 kDa ceramic membrane was used (1 Da = 1 g L^{-1} or a pore size less than 1 nm) that ensures ILs could not enter the pores. The stainless-steel carter is used to stabilize ILM and connect the system. The VOCs sensor (Ametek Mocon) is a photoionization detector (PID sensor), and the accuracy of this sensor is ±10%. The method to prepare an ILM has been described in the previous study [37].

Different concentrations of toluene with different flow rates were generated by the gas dilution system purchased from Omicron technologies (Eybens, France). As shown in Fig. 2, in the thermostatically controlled chamber, there are two ways for the gas mixture. First, the mixed gas goes to VOCs sensor to check gas sensor performance. Second, the mixed gas passes through the ILM and then goes to VOCs gas sensor

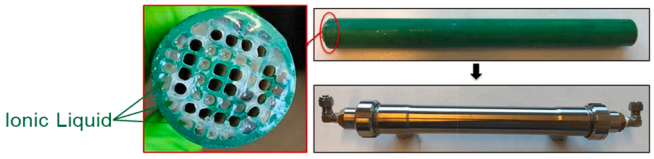

Fig. 1. The photos of the ILM and the stainless-steel carter [37].

to investigate the ILM performance. The toluene concentration inlet keeps constant, and the outlet is measured every second by VOCs sensors. When the toluene concentration outlet is equal to that inlet, the ILM reaches its saturation absorption. Desorption experiments carry out with continuous dry air with absorption operating conditions. Desorption is complete in all the cases, that is, most of the toluene absorbed is desorbed at the absorption temperature without heating or vacuum. In order to compare the performance of the ILM for gas absorption, the variation of outlet concentration versus time was studied. The mass of gas absorbed by the ILM can be calculated by the following equation:

$$m_{absorbed} = \int_0^t Q_g(C_{in} - C_{out})dt \quad (1)$$

where Q_g is the flow rate (L min^{-1}), $m_{absorbed}$ is the amount of absorbed by ILM (mg), C_{in} and C_{out} are the inlet and outlet concentration of toluene in the gas flow (mg L^{-1}), t is the time (sec).

2.2. Mathematical treatment

The process of gas absorbed by the ILM could be described with two steps (Fig. 3). In step 1, gas molecules move from the vapor phase, pass through channel walls of the support membrane, and then be absorbed on the surface of ILs. During this step, we make the assumption that only surface sorption occurs (Langmuir model) [38,39]. In step 2, gas molecules move from the surface to the bulk ILs, and diffusion takes place (1D diffusion model) [40,41]. In fact, during step 2, the surface absorption and diffusion occur simultaneously. For simplification, the surface sorption was neglected for the whole step 2 process. Because the gas absorption from vapor to the surface is much faster than the diffusion, the gas sorption is mainly controlled by diffusion.

2.2.1. Langmuir adsorption model (Step 1)

The Langmuir model reflects the monolayer sorption, and the adsorbed layer is one molecule in thickness [42,43]. Langmuir refers to homogeneous adsorption and an equilibrium saturation point where once a molecule occupies a site, no further adsorption can occur [44–46]. Assumptions of the model are following: i) the surface containing the adsorbing sites is a perfect flat plane without corrugations; ii) the gas adsorbs into an immobile state; iii) all sites are equivalent; iv) each site can hold at most one molecule; v) there are no interactions between adsorbate molecules on adjacent sites. The gas vapor sorption by almost all of the ILMs as the function of time during the initial part is approximately linear [38]. In this case, a constant absorption rate (k_L) was assumed for the whole first step process. It means linear absorption kinetics was proposed for surface sorption step. The equation is expressed as

$$C_e/Q_e = 1/Q_m \times C_e + 1/(k_{L,1} \times Q_m) \quad (2)$$

$$C_e = C_0 - C_t \quad (3)$$

$$Q_e = k_L \times t + Q_0, t \le t_0 \quad (4)$$

where $k_{L,1}$ is the Langmuir adsorption rate constant related to the adsorption energy; C_t is the concentration of gas outlet of the ILM at each time (mg L^{-1}); C_e is the adsorbed concentration of gas by IL surface at each time (mg L^{-1}); C_0 is the initial gas concentration, which is constant in this system (mg L^{-1}); Q_e is the amount of target gas absorbed at each time (mg); Q_m is the max amount of target gas absorbed at saturation (mg); Q_0 is the quality of residual in ILM (mg); k_L is the adsorption rate (mg sec^{-1}); t is time (sec), t_0 is the time-dividing point (sec), which depends on the IL types and process conditions.

2.2.2. One-dimensional (1D) diffusion model (Step 2)

The 1D diffusion model was proposed to determine the binary diffusion for a gas dissolving into an IL, and the volume of the IL is

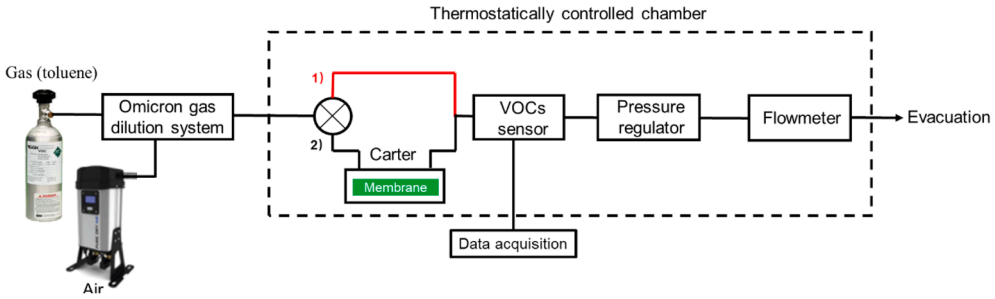

Fig. 2. The schematic diagram of VOCs removal process.

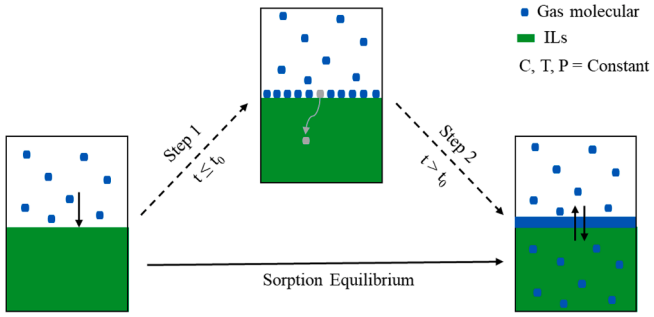

Fig. 3. Proposed two steps sorption mechanisms for gas sorption by the ILM [38].

constant during the process [41,47,48]. The basic assumptions of the model are following: i) no phase changing occur; ii) for one experiment the temperature and pressure remain constant (once gas dissolving occur, the system pressure and the IL density are constant); iii) the IL-gas system is a dilute solution where the thermophysical properties remain constant; iv) gas dissolves through a vertical diffusion process. 1D mass diffusion can be expressed as follows:

$$\partial C/\partial t = D \times (\partial^2 C/\partial z^2) \tag{5}$$

initial condition: $C = C_0$, when $t = 0$, and $0 < z < L$;
boundary conditions: $C = C_s$, when $t > 0$, $z = 0$;

$\partial C/\partial z = 0$, at $z = L$.

The quantity of gas dissolved at a specified time is the total mass of dissolved gas in the IL and not the mass profile in the *z*-axis. The mass of dissolved gas at a given time can be express:

$$C_m = C_s \times [1 - 2(1 - C_0/C_s) \times \sum_{n=0}^{\infty} \exp(-\lambda_n^2 \times D \times t)/L^2 \times \lambda_n^2], t > t_0 \tag{6}$$

where C_m is mass of target gas absorbed by per gram of ILs at each time (mg-toluene g-IL^{-1}), C_0 is the initial concentration (Q_m in Step 1) (mg-toluene g-IL^{-1}), C_s is the saturate mass of target gas absorbed by per gram of ILs (mg-toluene g-IL^{-1}) ($C_m \leq C_s$), D is the diffusion coefficient of gas vapor in the selected IL at operational conditions (m^2 s^{-1}), t is time (s), L is the height of IL in one channel of ILM (m) (Fig. 4). $\lambda = (n + 1/2)*\pi/L$ (n = 15 for convergence, the summation in C_s will less than 10^{-12}): this equation is an infinite summation, only initial time periods are sufficient in applications [47]).

It should be mentioned that the support membrane is nonwetted, which means pores of the support membrane full of gases. The toluene sorption by the ILM as a function of time during the first period (step 1) is approximately linear ($Q_e = k_L \times t + Q_0, t \leq t_0$). During step 2, the diffusion of toluene into the IL depended on the physicochemical properties (e.g., viscosity and solubility of the IL) and operating conditions (e.g., temperature). Based on this hypothesis, the step 2 ($C_m = C_s \times [1 - 2(1 - C_0/C_s) \times \sum_{n=0}^{\infty}\exp(-\lambda_n^2 \times D \times t)/L^2 \times \lambda_n^2], t > t_0$) is much slower than step 1 (a linear function). Because the toluene adsorbing from the gas phase to the surface is fast compared to the diffusion in the liquid phase, the toluene sorption is mainly controlled by diffusion. The time used in the two steps varies for different gases and ILs.

The gas diffusion coefficient in ILs can be described as following the Wilke-Chang equation [30]:

$$D_{gas-IL} = 7.4 \times 10^{-8} \times (\varnothing \times M_{IL})^{0.25} \times T/\mu_{IL} \times V_{gas}{}^{0.6} \tag{7}$$

where $D_{gas\text{-}IL}$ is the diffusivity (m^2 s^{-1}), T is the temperature (K), M_{IL} is the molar mass of the IL (g mol^{-1}), μ_{IL} is the viscosity of IL (mPa s), V_m is the molar volumes (cm^3 mol^{-1}), $\varnothing$ is the association parameter ($\varnothing$ =1, because IL acts as unassociated solvents).

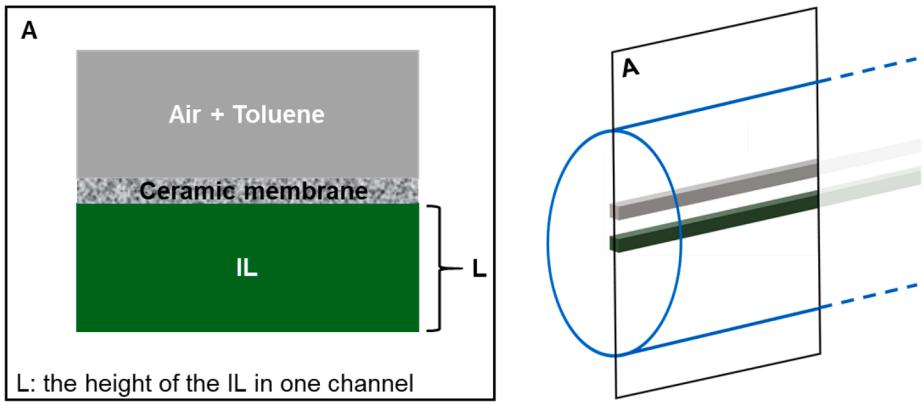

Fig. 4. The diagram of liquid sorbents height in the ILM.

3. Effects of operating parameters on toluene absorption by the ILM

In this study, the selected IL was used as a physical absorbent to capture toluene from the gas stream. The ceramic membrane acts as a support membrane. The absorption performance of toluene by the ILM was investigated by studying the influences of variable operating parameters, including the concentration of toluene inlet, flow rate, system pressure and temperature. Moreover, the sorption mechanism for toluene absorption by ILMs on different operation conditions was discussed. Toluene absorption by ILMs was simulated with two steps model following simulations: i) absorption of toluene by the IL is a physical absorption process; ii) the diffusion coefficients of toluene into the selected IL were calculated by the Wilke-Chang equation [30]. The modeled results were obtained by nonlinear regression fitting experimental data at given operating conditions.

3.1. Effect of the concentration of toluene inlet

Fig. 5 showed the effects of the initial concentration of toluene on the absorptivity at 1.07 atm, 20 °C and a flow rate of 0.30 L min^{-1}. Increased inlet concentration enhances membrane uptake of toluene for the same time before the membrane saturated. According to Fig. 5(a), the absorption process can be divided into two stages. First, toluene passes through the porous support membrane very fast. This stage was exhibited that the toluene concentration outlet of the ILM increasing rapidly. Second, the absorption went to a slow stage, which showed in the concentration outlet of ILM increasing slowly. At the experiment stop time (Fig. 5(b)), the ILM at 50 ppm of toluene almost reached a relatively stable stage, whereas the same ILM at 70 ppm still had a clear rising trend. In the gas–liquid absorption process, a toluene film (gas phase) and an IL film (liquid phase) were formed on the interface based on two-film theory [49]. Toluene must pass through these films to be dissolved into the bulk IL. The concentration gradient of the interface was increased with toluene concentration increasing due to higher concentration providing a higher driving force. This effect was favorable for the toluene absorption in an IL. When temperature and pressure were constants, the absorption capacity of toluene should be the same for the same quantity of [Bmim][NTf_2]. Therefore, higher concentration inlet resulted in more quantity of toluene reached the bulk IL and was absorbed during the same time. It should be mentioned that the ILM under 50 ppm absorbed toluene very slowly compared to under 70 ppm at the experiment stop time. Normally, higher toluene concentration in the gas phase was high results a higher concentration in liquid phase own to vapor–liquid equilibrium. There are two other assumptions proposed based on this result: i) the ILM under 50 ppm stop absorbing toluene at experiment stop time, but not all IL worked during this process: the IL in the center of channels might not absorb toluene; ii) the ILM under 50 ppm of toluene still absorbing toluene at experiment stop time, but the absorption rate was very slow, which could not be exhibited clearly on the figure. For the surface adsorption (step 1), toluene molecules passed through the porous ceramic membrane and reached the IL surface. As Table 2 shown, a higher concentration of toluene inlet resulted in a faster surface adsorption rate (k_L) because of a higher driving force provided. Therefore, it was clear that the first step took a long time with lower concentration inlet. For gas diffusion into the liquid phase (step 2), this step was the rate control step. The diffusion coefficient was a key parameter for the second step. According to the Wilke-Chang equation, the diffusion coefficient of toluene into ILs was influenced by the temperature and pressure [30]. From Fig. 5(b), the modeled results were fitted well on experimental results, and it demonstrated that the diffusion coefficient was not affected by concentrations. It was observed that ILM absorbed toluene much faster with higher concentration inlet, because the increasing concentration of toluene inlet, the mass transfer resistance of the liquid phase was reduced. In conclusion, the absorption performance of ILM with higher concentration inlet was better. Considering the measuring range of VOCs sensor used, 70 ppm of toluene inlet was selected for the optimized experiment.

3.2. Effect of gas flow rate

The effect of different flow rates from 0.10, 0.15 to 0.30 L min^{-1} was studied. The flow rate of gas passing was measured by a digital flowmeter in the input and output of the ILM. The values are similar. From Fig. 6(a), there was a distinct downtrend for the concentration of the toluene outlet with the acceleration of the flow rate. This result indicated that absorptivity significantly influenced by the contact time between the toluene and the IL. At high flow rate, toluene may be blown out without fully contacting with the IL. From the total mass of toluene absorbed by ILM as a function of time (Fig. 6(b)), during the same time and before the ILM saturation, the membrane with a higher flow rate absorbed more quantity of toluene. The higher flow rate could enhance the toluene absorption rate because of the higher mass of the toluene inlet (higher concentration gradient) during the same time. The surface adsorption parameters from the Langmuir model were shown in Table 3. It observed that the surface sorption rate was enhanced with a higher gas flow rate. For our ILM geometry, the influences of the quantity of toluene inlet have a dominant role compared to contact time reduction. Therefore, the time consumption of surface adsorption was greatly reduced. It was confirmed that the toluene adsorption rate was increased

Table 2
The surface sorption parameters of different concentrations inlet.

Concentration (ppm)	Mass of toluene inlet (mg min^{-1})	k_L	Q_m (mg-toluene g-IL^{-1})	t (min)	R^2
70	0.085	0.0012	0.17	2.33	0.990
50	0.063	0.0004	0.11	4.50	0.992

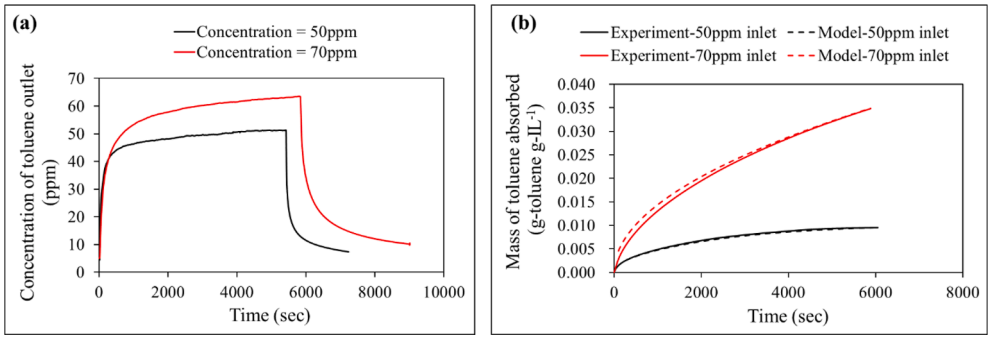

Fig. 5. (a) Effects of inlet toluene concentration on ILM absorption performance; (b) Mass of toluene absorbed by ILM with different inlet toluene concentration. ([Bmim][NTf_2], The concentration of toluene inlet = 50 / 70 ppm, Flow rate = 0.30 L min^{-1}, P = 1.07 atm, T = 20 °C).

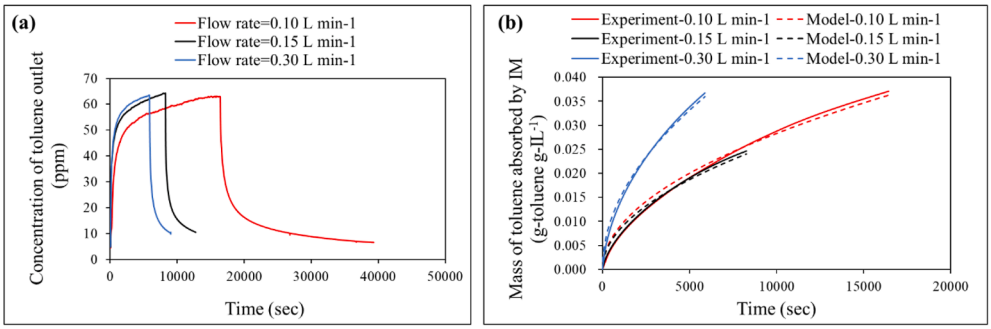

Fig. 6. (a) Effects of different flow rates on ILM absorption performance; (b) Total mass of toluene absorbed by ILM with different flow rates. ([Bmim][NTf_2], The concentration of toluene inlet = 70 ppm, Flow rate = 0.10 / 0.15/ 0.30 L min^{-1}, P = 1.07 atm, T = 20 °C).

Table 3
The surface sorption parameters of different flow rates.

Flow rate (L $min^{-1)}$	Mass of toluene inlet (mg min^{-1})	k_L	Q_m (mg-toluene g-IL^{-1})	t (min)	R^2
0.10	0.028	0.0003	0.15	8.33	0.983
0.15	0.042	0.0004	0.14	5.83	0.982
0.30	0.085	0.0012	0.17	2.33	0.986

Table 4
The surface sorption parameters of different pressures.

Pressure (atm)	Mass of toluene inlet (mg min^{-1})	k_L	Q_m (mg-toluene g-IL^{-1})	t (min)	R^2
1.07	0.085	0.0012	0.17	2.33	0.990
1.12	0.089	0.0012	0.19	2.63	0.989
1.17	0.093	0.0012	0.21	2.91	0.990

with flow rate increasing from 0.10 to 0.30 L min^{-1}. The diffusion coefficient of toluene was not affected by the gas flow rate based on simulated results. During the same time and before the ILM saturation, a higher flow rate inlet resulted in higher mass absorbed.

3.3. *Effect of pressure*

Pressure for the gas phase is a crucial factor for ILM due to the gas–liquid absorption mechanism. Experiments were performed on the ILM in the operating conditions of 20 °C, gas flow rate of 0.30 L min^{-1}, pressure from 1.07 to 1.17 atm. The experimental results were (Fig. 7) showed that pressure significantly influenced the mass transfer. The membrane flux depended on the mass transfer coefficient and the driving force (△P) [50]. When increase pressure, the driving force was increased, thus membrane flux boosted. As operating conditions, for one same ILM, the absorption capacity was constant due to the same quantity of the IL used. According to the mass of toluene absorbed by the ILM under different pressures, higher pressure brought a faster absorption rate owing to reaching the same absorption capacity of the ILM at a shorter time consumed. Therefore, higher pressure has a positive effect on toluene absorbing by the ILM. From Fig. 7(b), higher pressure provided a higher driving force, which pushed the more quantity of toluene into the IL bulk. For surface adsorption (step 1), Table 4 showed that the higher pressure increased the surface sorption capacities, but the sorption rates kept constant. The ILM took a longer time in surface adsorption with a higher pressure. However, it was inversed in diffusion. For diffusion (step 2), Fig. 7(b) gave the tendency of toluene gas diffusion into [Bmim][NTf_2] bulk with different pressures. When P = 1.17 atm, at the beginning of diffusion, the modeled line was not in good agreement with the experimental result: it could be the reason that higher pressure results over-saturated surface adsorption and excessed toluene vapors cannot be diffusion into the bulk IL efficiently. Therefore, parts of toluene vapors desorbed from the surface of the IL and exit [51]. When the pressure increased 0.10 atm (from 1.07 to 1.17 atm), for the same duration, the absorption mass increased from 129.46 to 219.07 mg-toluene g-IL^{-1} with the slightly increasing of diffusion coefficient. Higher pressure has a positive effect on toluene removal by the ILM based on experimental and modeled results. However, it should not be ignored that the increasing pressure also could push the IL into porous of the ceramic membrane resulting in leakage. In this work, it is impossible for the IL to enter the porous of the ceramic membrane: the critical pressure of the porous membrane can be calculated based on the Young-Laplace equation [52]. According to the contact angle between the IL and the ceramic membrane, surface tension of the IL and pore size of the ceramic membrane, the critical entry pressure is very large (higher than 10 atm). Among all experiments, the operating pressure was lower than the critical entry pressure, which indicated that the IL could not enter

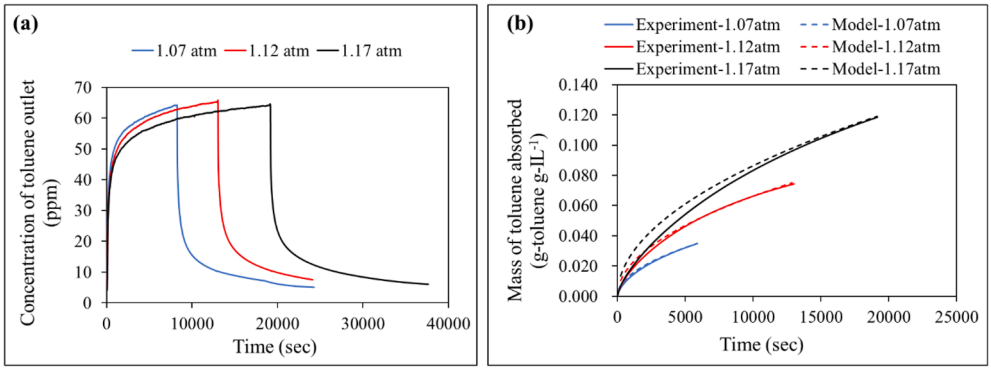

Fig. 7. (a) Effects of different pressures on ILM absorption performance; (b) Mass of toluene absorbed by ILM with different pressures. ([Bmim][NTf_2], The concentration of toluene inlet = 70 ppm, Flow rate = 0.30 L min^{-1}, P = 1.07 / 1.12 / 1.17 atm, T = 20 °C).

the porous of the ceramic membrane.

3.4. Effect of temperature

Temperature is a key factor in removal efficiency for toluene removal by the ILM. The effect of temperature was investigated from 20 to 60 °C. From Fig. 8(a), there was no significant effect of temperature on toluene removal by the ILM in our testing range. However, from Fig. 8(b), the amount of toluene absorbed by the ILM increased with decreasing temperature. The temperature has a negative effect on toluene removal, which has been confirmed by several studies [30,53,54]. This is agreed by Henry's law that solubility of gases usually decreases with increasing temperature. Faghihi-Zarandi et al. [55] showed that the absorption capacity was increased from 0 to 20 °C. For the temperature range from 20 to 60 °C, the toluene removal efficiency and absorption capacity by ILs were a little bit reduced by temperature increasing. However, when temperature increased from 60 to 120 °C, the toluene absorption capacities by ILs was decreased sharply because the physical interactions between toluene and the IL such as hydrogen bonds and hydrophobic interaction were decreased in high temperature. Moreover, some physical properties of ILs were strongly influenced by temperature. For example, for a pressure of 1 atm, increasing temperature from 20, 40 to 60 °C could reduce the viscosity of [Bmim][NTf_2] from 62.0, 27.8 to 15.1 mPa s respectively. Furthermore, a higher viscosity (lower temperature) resulted in a lower gas diffusion coefficient and consequently, higher liquid phase mass transfer resistance [51,56–58].

From Table 5, the surface sorption parameters showed that the surface equilibrium concentration was slightly increased. At the same time, the surface adsorption rate also enhanced with temperature increasing due to the toluene molecular motion increasing. From the gas diffusion into liquid bulk (step 2), it is observed that the effect of temperature on toluene absorption was negative. When the temperature increased from 20 to 60 °C, the diffusion coefficient was increased while the absorption capacity (gas solubility) was decreased. The differences in the toluene concentration outlet of the ILM over the testing temperature range were not large because the temperature effect on toluene removal was limited. The influence of gas solubility plays a dominant role. Therefore, the optimized temperature selected should consider based on both gas solubility and the viscosity of the liquid sorbent.

4. Toluene absorbed by the ILM: The case of optimal conditions

According to the above results, the toluene absorbed by an ILM at proposed operating conditions was studied on the experiment. The proposed operating conditions are the concentration of toluene ($C_{toluene}$) in gas stream = 70 ppm, Flow rate = 0.10 L min^{-1}, Pressure = 1.17 atm, Temperature = 20 °C. From Fig. 9(a), the concentration of the toluene outlet of the ILM increased with time going. Around 32 h, the concentration of the toluene outlet was stable at the range from 63 to 64 ppm.

Table 5
The surface sorption parameters of different temperatures.

Temperature (°C)	Mass of toluene inlet (mg min^{-1})	k_L	Q_m (mg-toluene g-IL^{-1})	t (min)	R^2
20	0.085	0.0012	0.17	2.33	0.990
40	0.079	0.0013	0.20	2.50	0.995
60	0.075	0.0015	0.22	2.45	0.991

Considering the accuracy of the VOCs sensor (±10%), the ILM could be regarded as saturation. In addition, as Fig. 9(b) shown, the mass of toluene absorbed increased 0.22 mg-toluene g^{-1} of the IL from 31 to 32 h (1 h). While this value only increased 0.04 mg-toluene g^{-1} of the IL from 32 to 33 h (1 h). Furthermore, from 33 to 64 h (31 h), the mass of toluene absorbed by the ILM was 0.05 mg-toluene g^{-1} of the IL. These results also demonstrated the ILM was near saturation.

The modeled results (Fig. 9(b)) were agreed experimental results, both surface adsorption (Step 1) and diffusion (Step 2). From the insert figure (step 1), the surface adsorption rate (k_L) was 0.0008, which was higher than 0.10 L min^{-1} gas flow rate and 1.07 atm (k_L = 0.0003) but lower than 0.30 L min^{-1} gas flow rate and 1.17 atm (k_L = 0.0012). This result indicated that the gas flow rate played a relatively important role than the system pressure. The surface equilibrium concentration (Q_m) was 24.96 mg-toluene g-IL^{-1}. For gas diffusion into the bulk IL (Step 2), the diffusion coefficient ($D_{toluene\text{-}IL}$) was 4.12*10^{-11} m^2 s^{-1}, which was the same with 1.07 atm and 20 °C because this value was depended on temperature and pressure. At proposed operating conditions, the ILM needed 31.47 h to reach its saturation, and the saturated mass of toluene captured by the ILM was around 224.74 mg g^{-1} of [Bmim][NTf_2]. Wang et al. [54] studied results showed that the toluene absorption capacity by [Bmim][NTf_2] was 140 mg g^{-1} of the IL at 20 °C and 1 atm. Moreover, Bedia et al. [30] indicated the toluene absorption capacity of [Bmim][NTf_2] was around 210 mg g^{-1} of [Bmim][NTf_2] at same operating conditions based on both experimental data and computational analysis. From this work, the toluene absorption capacity was 224.47 mg g^{-1} of the selected IL, which is in agreement with Bedia's research. Thus, the [Bmim][NTf_2] is a promising liquid sorbent for toluene removal.

5. Conclusion

Recently, ILs are attracting more and more attention to gas separation due to their excellent properties. However, some studies underlined that there are some environmental risks of ILs, which limits their applications in industrial processes. The ILM provides a new pathway to prevent ILs from environmental risks in gas separation processes. Based on the high absorption capacities, [Bmim][NTf_2] was selected as an absorbent combining with a ceramic membrane for toluene removal. In addition, the ILM was investigated by experiment and modeling based on different operating conditions, including the concentration of toluene

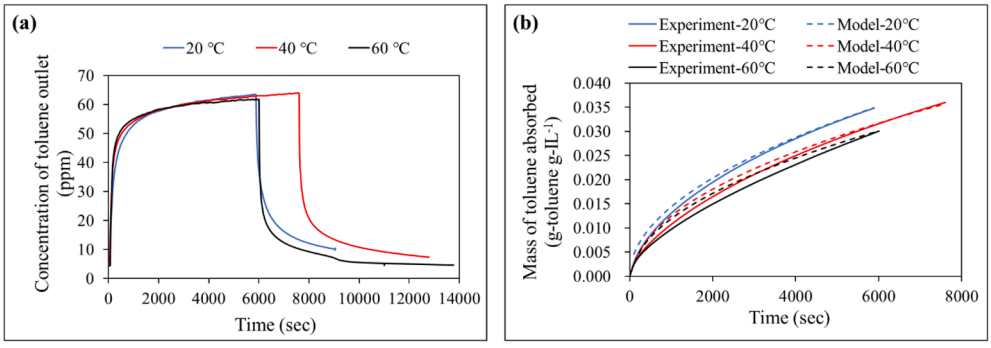

Fig. 8. (a) Effects of different temperatures on ILM absorption performance; (b) Mass of toluene absorbed by ILM with different temperatures. ([Bmim][NTf_2], The concentration of toluene inlet = 70 ppm, Flow rate = 0.30 L min^{-1}, P = 1.07 atm, T = 20/40/60 °C).

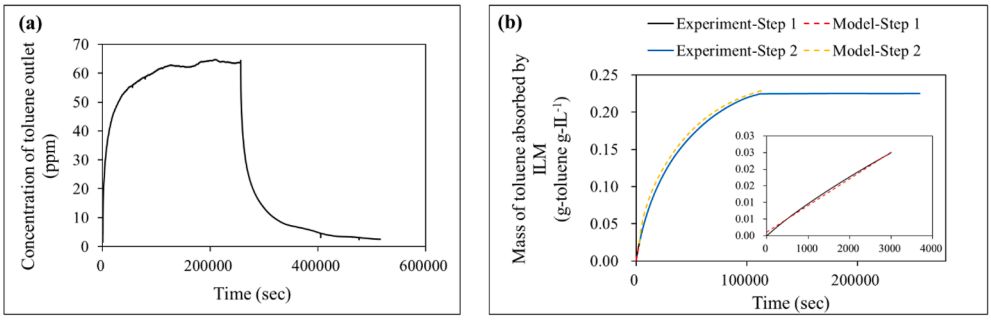

Fig. 9. (a) Absorption of toluene at proposed operating conditions; (b) Mass of toluene absorbed by ILM at proposed operating conditions: experimental and simulated results. The insert figure is the Langmuir model (step 1) result. ([Bmim][NTf_2], The concentration of toluene inlet = 70 ppm, Flow rate = 0.10 L min^{-1}, P = 1.17 atm, T = 20 °C).

inlet, gas flow rate, system pressure and temperature. A comprehensive two steps model was used to simulate the gas absorption process of the ILM with nonwetted conditions. Results demonstrated that higher concentration boosts the mass transfer due to a higher concentration gradient. Flow rate influenced the contact time between the toluene and the IL. ILM removal efficiency was enhanced with the flow rate increasing. Higher pressure provided a higher driving force to enhance toluene absorption. The temperature could influence both gas absorption and the viscosity of the IL. The lower temperature was a benefit for gas absorption on liquid absorbent, however, increase the viscosity of the IL, which resistance the mass transfer. The modeling results explained that the absorption process was involved in two steps: surface adsorption and diffusion. For the surface adsorption (step 1), the dynamic equilibrium concentration was around 0.18 mg-toluene per gram of the IL, which was not affected by the operating conditions as expected. For the diffusion (step 2), the ILM absorption capacity of toluene was calculated around 224.47 mg-toluene g-IL^{-1} using [Bmim][NTf_2] as a liquid sorbent. This value is in agreement with the state of the art. Above all, the ILM can effectively reduce the possibilities of environmental risks from ILs because the ceramic membrane can prevent ILs leakage and protect ILs from solid suspension in the gas phase. It provides a promising method for using ILs as absorbents for purification of exhaust gas.

Funding source

The authors want to thank China Scholarship Council (CSC) for partial financial support.

Declaration of Competing Interest

The authors declare that they have no known competing financial interests or personal relationships that could have appeared to influence the work reported in this paper.

Acknowledgments

The authors would like to acknowledge China Scholarship Council for partial financial support (201701810017). The authors are very grateful to Soilihi Moindjie for his technical support for test bench setup. The authors are very grateful to Tianqi Song (MeCA, INT, Aix Marseille Univ.) for his suggestion on Python codes. The authors are also very grateful to Mark B. Shiflett (University of Kansas) for his kind answers to our questions.

References

[1] V. Soni, P. Singh, V. Shree, V. Goel, Effects of VOCs on Human Health, in: N. Sharma, A.K. Agarwal, P. Eastwood, T. Gupta, A.P. Singh (Eds.), Air Pollut. Control, Springer, Singapore, 2018: pp. 119–142. https://doi.org/10.1007/978-981-10-7185-0_8.

[2] C. Lyu, S.L. Capps, A. Hakami, S. Zhao, J. Resler, G.R. Carmichael, A. Sandu, A. G. Russell, T. Chai, D.K. Henze, Elucidating emissions control strategies for ozone to protect human health and public welfare within the continental United States, Environ. Res. Lett. 14 (2019), 124093, https://doi.org/10.1088/1748-9326/ab5e05.

[3] G. Li, W. Wei, X. Shao, L. Nie, H. Wang, X. Yan, R. Zhang, A comprehensive classification method for VOC emission sources to tackle air pollution based on VOC species reactivity and emission amounts, J. Environ. Sci. 67 (2018) 78–88, https://doi.org/10.1016/j.jes.2017.08.003.

[4] L. Zhu, D. Shen, K.H. Luo, A critical review on VOCs adsorption by different porous materials: species, mechanisms and modification methods, J. Hazard. Mater. 389 (2020), 122102, https://doi.org/10.1016/j.jhazmat.2020.122102.

[5] S. Liu, Y. Peng, J. Chen, T. Yan, Y. Zhang, J. Liu, J. Li, A new insight into adsorption state and mechanism of adsorbates in porous materials, J. Hazard. Mater. 382 (2020), 121103, https://doi.org/10.1016/j.jhazmat.2019.121103.

[6] B. Belaissaoui, Y. Le Moullec, E. Favre, Energy efficiency of a hybrid membrane/condensation process for VOC (Volatile Organic Compounds) recovery from air: a generic approach, Energy. 95 (2016) 291–302, https://doi.org/10.1016/j.energy.2015.12.006.

[7] N.N.R. Ahmad, C.P. Leo, A.W. Mohammad, A.L. Ahmad, Interfacial sealing and functionalization of polysulfone/SAPO-34 mixed matrix membrane using acetate-based ionic liquid in post-impregnation for CO_2 capture, Sep. Purif. Technol. 197 (2018) 439–448, https://doi.org/10.1016/j.seppur.2017.12.054.

[8] X. Yan, S. Anguille, M. Bendahan, P. Moulin, Ionic liquids combined with membrane separation processes: a review, Sep. Purif. Technol. 222 (2019) 230–253, https://doi.org/10.1016/j.seppur.2019.03.103.

[9] X. Li, J. Ma, X. Ling, Design and dynamic behaviour investigation of a novel VOC recovery system based on a deep condensation process, Cryogenics 107 (2020), 103060, https://doi.org/10.1016/j.cryogenics.2020.103060.

[10] N. Ayrilmis, T. Kapti, A. Gürel, M. Ohlmeyer, Effect of wood-drying condensate on emission of volatile organic compounds and bonding properties of fibreboard, J. Bionic Eng. 17 (2020) 206–214, https://doi.org/10.1007/s42235-020-0016-5.

[11] T. Uragami, Y. Matsuoka, T. Miyata, Permeation and separation characteristics in removal of dilute volatile organic compounds from aqueous solutions through copolymer membranes consisted of poly(styrene) and poly(dimethylsiloxane) containing a hydrophobic ionic liquid by pervaporation, J. Membr. Sci. 506 (2016) 109–118, https://doi.org/10.1016/j.memsci.2016.01.031.

[12] V.M. Ortiz-Martínez, M.J. Salar-García, Chapter 4 - Separation of volatile organic compounds by using immobilized ionic liquids, in: Inamuddin, A.M. Asiri, S. Kanchi (Eds.), Green Sustain. Process Chem. Environ. Eng. Sci., Elsevier, 2020: pp. 105–122. https://doi.org/10.1016/B978-0-12-817386-2.00004-4.

[13] M.K. Mondal, H.K. Balsora, P. Varshney, Progress and trends in CO_2 capture/separation technologies: a review, Energy. 46 (2012) 431–441, https://doi.org/10.1016/j.energy.2012.08.006.

[14] C. Wang, H. Yin, P. Tian, X. Sun, X. Pan, K. Chen, W.-J. Chen, Q.-H. Wu, S. Luo, Remarkable adsorption performance of MOF-199 derived porous carbons for benzene vapor, Environ. Res. 184 (2020), 109323, https://doi.org/10.1016/j.envres.2020.109323.

[15] W.-Q. Xu, S. He, C.-C. Lin, Y.-X. Qiu, X.-J. Liu, T. Jiang, W.-T. Liu, X.-L. Zhang, J.-J. Jiang, A copper based metal-organic framework: synthesis, modification and VOCs adsorption, Inorg. Chem. Commun. 92 (2018) 1–4, https://doi.org/10.1016/j.inoche.2018.03.024.

[16] M. Shafiei, M.S. Alivand, A. Rashidi, A. Samimi, D. Mohebbi-Kalhori, Synthesis and adsorption performance of a modified micro-mesoporous MIL-101(Cr) for VOCs removal at ambient conditions, Chem. Eng. J. 341 (2018) 164–174, https://doi.org/10.1016/j.cej.2018.02.027.

[17] J. Qi, J. Li, Y. Li, X. Fang, X. Sun, J. Shen, W. Han, L. Wang, Synthesis of porous carbon beads with controllable pore structure for volatile organic compounds removal, Chem. Eng. J. 307 (2017) 989–998, https://doi.org/10.1016/j.cej.2016.09.022.

[18] B. Satilmis, T. Uyar, Electrospinning of ultrafine poly(1-trimethylsilyl-1-propyne) [PTMSP] fibers: highly porous fibrous membranes for volatile organic compound removal, ACS Appl. Polym. Mater. 1 (2019) 787–796, https://doi.org/10.1021/acsapm.9b00027.

[19] H. Liu, Y. Yu, Q. Shao, C. Long, Porous polymeric resin for adsorbing low concentration of VOCs: unveiling adsorption mechanism and effect of VOCs' molecular properties, Sep. Purif. Technol. 228 (2019), 115755, https://doi.org/10.1016/j.seppur.2019.115755.

[20] A. Ikhlaq, B. Kasprzyk-Hordern, Catalytic ozonation of chlorinated VOCs on ZSM-5 zeolites and alumina: Formation of chlorides, Appl. Catal. B Environ. 200 (2017) 274–282, https://doi.org/10.1016/j.apcatb.2016.07.019.

[21] C. Megías-Sayago, I. Lara-Ibeas, Q. Wang, S. Le Calvé, B. Louis, Volatile organic compounds (VOCs) removal capacity of ZSM-5 zeolite adsorbents for near real-time BTEX detection, J. Environ. Chem. Eng. 8 (2020), 103724, https://doi.org/10.1016/j.jece.2020.103724.

[22] M. Wołowiec, B. Muir, K. Zięba, T. Bajda, M. Kowalik, W. Franus, Experimental study on the removal of VOCs and PAHs by zeolites and surfactant-modified zeolites, Energy Fuels. 31 (2017) 8803–8812, https://doi.org/10.1021/acs.energyfuels.7b01124.

[23] R. Hariz, J.I. del Rio Sanz, C. Mercier, R. Valentin, N. Dietrich, Z. Mouloungui, G. Hébrard, Absorption of toluene by vegetable oil–water emulsion in scrubbing tower: experiments and modeling, Chem. Eng. Sci. 157 (2017) 264–271, https://doi.org/10.1016/j.ces.2016.06.008.

[24] Y. Long, S. Wu, Y. Xiao, P. Cui, H. Zhou, VOCs reduction and inhibition mechanisms of using active carbon filler in bituminous materials, J. Clean. Prod. 181 (2018) 784–793, https://doi.org/10.1016/j.jclepro.2018.01.222.

[25] E. Hunter-Sellars, J.J. Tee, I.P. Parkin, D.R. Williams, Adsorption of volatile organic compounds by industrial porous materials: impact of relative humidity, Microporous Mesoporous Mater. 298 (2020), 110090, https://doi.org/10.1016/j.micromeso.2020.110090.

[26] L. Ma, M. He, P. Fu, X. Jiang, W. Lv, Y. Huang, Y. Liu, H. Wang, Adsorption of volatile organic compounds on modified spherical activated carbon in a new cyclonic fluidized bed, Sep. Purif. Technol. 235 (2020), 116146, https://doi.org/10.1016/j.seppur.2019.116146.

[27] C. Zhou, Y. Zhan, S. Chen, M. Xia, C. Ronda, M. Sun, H. Chen, X. Shen, Combined effects of temperature and humidity on indoor VOCs pollution: Intercity comparison, Build. Environ. 121 (2017) 26–34, https://doi.org/10.1016/j.buildenv.2017.04.013.

[28] E.J. Park, H.O. Seo, Y.D. Kim, Influence of humidity on the removal of volatile organic compounds using solid surfaces, Catal. Today. 295 (2017) 3–13, https://doi.org/10.1016/j.cattod.2017.02.036.

[29] J. Xu, J.S. Zhang, An experimental study of relative humidity effect on VOCs' effective diffusion coefficient and partition coefficient in a porous medium, Build. Environ. 46 (2011) 1785–1796, https://doi.org/10.1016/j.buildenv.2011.02.007.

[30] J. Bedia, E. Ruiz, J. de Riva, V.R. Ferro, J. Palomar, J.J. Rodriguez, Optimized ionic liquids for toluene absorption, AIChE J. 59 (2013) 1648–1656, https://doi.org/10.1002/aic.13926.

[31] N. Tandjaoui, M. Abouseoud, A. Couvert, A. Amrane, A. Tassist, A combination of absorption and enzymatic biodegradation: phenol elimination from aqueous and organic phase, Environ. Technol. 40 (2019) 625–632, https://doi.org/10.1080/09593330.2017.1400110.

[32] A.-S. Rodriguez Castillo, P.-F. Biard, S. Guihéneuf, L. Paquin, A. Amrane, A. Couvert, Assessment of VOC absorption in hydrophobic ionic liquids: Measurement of partition and diffusion coefficients and simulation of a packed column, Chem. Eng. J. 360 (2019) 1416–1426, https://doi.org/10.1016/j.cej.2018.10.146.

[33] T. Gutel, C.C. Santini, A.A.H. Pádua, B. Fenet, Y. Chauvin, J.N. Canongia Lopes, F. Bayard, M.F. Costa Gomes, A.S. Pensado, Interaction between the π-system of toluene and the imidazolium ring of ionic liquids: a combined NMR and molecular simulation study, J. Phys. Chem. B. 113 (2009) 170–177, https://doi.org/10.1021/jp805573t.

[34] H. Cheng, Y. Sun, X. Wang, S. Zou, G. Ye, H. Huang, D. Ye, Hierarchical porous carbon fabricated from cellulose-degrading fungus modified rice husks: ultrahigh surface area and impressive improvement in toluene adsorption, J. Hazard. Mater. 392 (2020), 122298, https://doi.org/10.1016/j.jhazmat.2020.122298.

[35] G. Gregis, S. Schaefer, J.-B. Sanchez, V. Fierro, F. Berger, I. Bezverkhyy, G. Weber, J.-P. Bellat, A. Celzard, Characterization of materials toward toluene traces detection for air quality monitoring and lung cancer diagnosis, Mater. Chem. Phys. 192 (2017) 374–382, https://doi.org/10.1016/j.matchemphys.2017.02.015.

[36] R. Ghidossi, E. Carretier, D. Veyret, D. Dhaler, P. Moulin, Optimizing the compacity of ceramic membranes, J. Membr. Sci. 360 (2010) 483–492, https://doi.org/10.1016/j.memsci.2010.05.050.

[37] X. Yan, A. Favard, S. Anguille, M. Bendahan, P. Moulin, Effects of operating parameters on ionic liquid membrane to remove humidity in a green continuous process, Membranes. 9 (2019) 65, https://doi.org/10.3390/membranes9050065.

[38] Y. Cao, Y. Chen, X. Sun, Z. Zhang, T. Mu, Water sorption in ionic liquids: kinetics, mechanisms and hydrophilicity, Phys. Chem. Chem. Phys. 14 (2012) 12252–12262, https://doi.org/10.1039/C2CP41798G.

[39] Y. Cao, Y. Chen, L. Lu, Z. Xue, T. Mu, Water sorption in functionalized ionic liquids: kinetics and intermolecular interactions, Ind. Eng. Chem. Res. 52 (2013) 2073–2083, https://doi.org/10.1021/ie302850z.

[40] Y. Chen, Y. Cao, C. Yan, Y. Zhang, T. Mu, The dynamic process of atmospheric water sorption in [BMIM][Ac]: quantifying bulk versus surface sorption and utilizing atmospheric water as a structure probe, J. Phys. Chem. B. 118 (2014) 6896–6907, https://doi.org/10.1021/jp502995k.

[41] M.A. Rocha, M.B. Shiflett, Water sorption and diffusivity in $[C_2C_1im][BF_4]$, $[C_4C_1im][OAc]$, and $[C_4C_1im][Cl]$, Ind. Eng. Chem. Res. 58 (2019) 1743–1753, https://doi.org/10.1021/acs.iecr.8b05689.

[42] M.Y.M. Abdelrahim, C.F. Martins, A. Luísa, C. Neves, C.T. Capasso, I.M. Supuran, J. G. Coelhoso, M.B. Crespo, Supported ionic liquid membranes immobilized with carbonic anhydrases for CO_2 transport at high temperatures, J. Membr. Sci. 528 (2017) 225–230, https://doi.org/10.1016/j.memsci.2017.01.033.

[43] I. Langmuir, The constitution and fundamental properties of solids and liquids. Part I. solids, J. Am. Chem. Soc. 38 (1916) 2221–2295, https://doi.org/10.1021/ja02268a002.

[44] K.Y. Foo, B.H. Hameed, Insights into the modeling of adsorption isotherm systems, Chem. Eng. J. 156 (2010) 2–10, https://doi.org/10.1016/j.cej.2009.09.013.

[45] A.M. Aljeboree, A.N. Alshirifi, A.F. Alkaim, Kinetics and equilibrium study for the adsorption of textile dyes on coconut shell activated carbon, Arab. J. Chem. 10 (2017) S3381–S3393, https://doi.org/10.1016/j.arabjc.2014.01.020.

[46] V. Saruchi, Kumar, Adsorption kinetics and isotherms for the removal of rhodamine B dye and Pb+2 ions from aqueous solutions by a hybrid ion-exchanger, Arab. J. Chem. 12 (2019) 316–329, https://doi.org/10.1016/j.arabjc.2016.11.009.

[47] M.B. Shiflett, A. Yokozeki, Solubilities and diffusivities of carbon dioxide in ionic liquids: [bmim][PF_6] and [bmim][BF_4], Ind. Eng. Chem. Res. 44 (2005) 4453–4464, https://doi.org/10.1021/ie058003d.

[48] R. Santiago, J. Lemus, D. Moreno, C. Moya, M. Larriba, N. Alonso-Morales, M. A. Gilarranz, J.J. Rodríguez, J. Palomar, From kinetics to equilibrium control in CO_2 capture columns using Encapsulated Ionic Liquids (ENILs), Chem. Eng. J. 348 (2018) 661–668, https://doi.org/10.1016/j.cej.2018.05.029.

[49] X. Ma, M. Wu, S. Liu, J. Huang, B. Sun, Y. Zhou, Q. Zhu, H. Lu, Concentration control of volatile organic compounds by ionic liquid absorption and desorption, Chin. J. Chem. Eng. 27 (2019) 2383–2389, https://doi.org/10.1016/j.cjche.2018.12.019.

[50] L. Zhang, B. Yan, X. Xiao, Toluene gas treatment by combination of ionic liquid absorption and photocatalytic oxidation, J. Environ. Chem. Eng. 5 (2017) 539–546, https://doi.org/10.1016/j.jece.2016.12.028.

[51] T. Koller, M.H. Rausch, P.S. Schulz, M. Berger, P. Wasserscheid, I.G. Economou, A. Leipertz, A.P. Fröba, Viscosity, interfacial tension, self-diffusion coefficient, density, and refractive index of the ionic liquid 1-ethyl-3-methylimidazolium tetracyanoborate as a function of temperature at atmospheric pressure, J. Chem. Eng. Data. 57 (2012) 828–835, https://doi.org/10.1021/je201080c.

[52] Z. Dai, L. Deng, Membrane absorption using ionic liquid for pre-combustion CO_2 capture at elevated pressure and temperature, Int. J. Greenh. Gas Control. 54 (2016) 59–69, https://doi.org/10.1016/j.ijggc.2016.09.001.

[53] M.-D. Vuong, A. Couvert, C. Couriol, A. Amrane, P. Le Cloirec, C. Renner, Determination of the Henry's constant and the mass transfer rate of VOCs in solvents, Chem. Eng. J. 150 (2009) 426–430, https://doi.org/10.1016/j.cej.2009.01.027.

[54] W. Wang, X. Ma, S. Grimes, H. Cai, M. Zhang, Study on the absorbability, regeneration characteristics and thermal stability of ionic liquids for VOCs removal, Chem. Eng. J. 328 (2017) 353–359, https://doi.org/10.1016/j.cej.2017.06.178.

[55] A. Faghihi-Zarandi, H. Shirkhanloo, C. Jamshidzadeh, A new method for removal of hazardous toluene vapor from air based on ionic liquid-phase adsorbent, Int. J. Environ. Sci. Technol. 16 (2019) 2797–2808, https://doi.org/10.1007/s13762-018-1975-5.

[56] Z. Dai, R.D. Noble, D.L. Gin, X. Zhang, L. Deng, Combination of ionic liquids with membrane technology: a new approach for CO2 separation, J. Membr. Sci. 497 (2016) 1–20, https://doi.org/10.1016/j.memsci.2015.08.060.

[57] J. Zhu, F. Xin, J. Huang, X. Dong, H. Liu, Adsorption and diffusivity of CO_2 in phosphonium ionic liquid modified silica, Chem. Eng. J. 246 (2014) 79–87, https://doi.org/10.1016/j.cej.2014.02.057.

[58] R. Fortunato, C.A.M. Afonso, M.A.M. Reis, J.G. Crespo, Supported liquid membranes using ionic liquids: study of stability and transport mechanisms, J. Membr. Sci. 242 (2004) 197–209, https://doi.org/10.1016/j.memsci.2003.07.028.